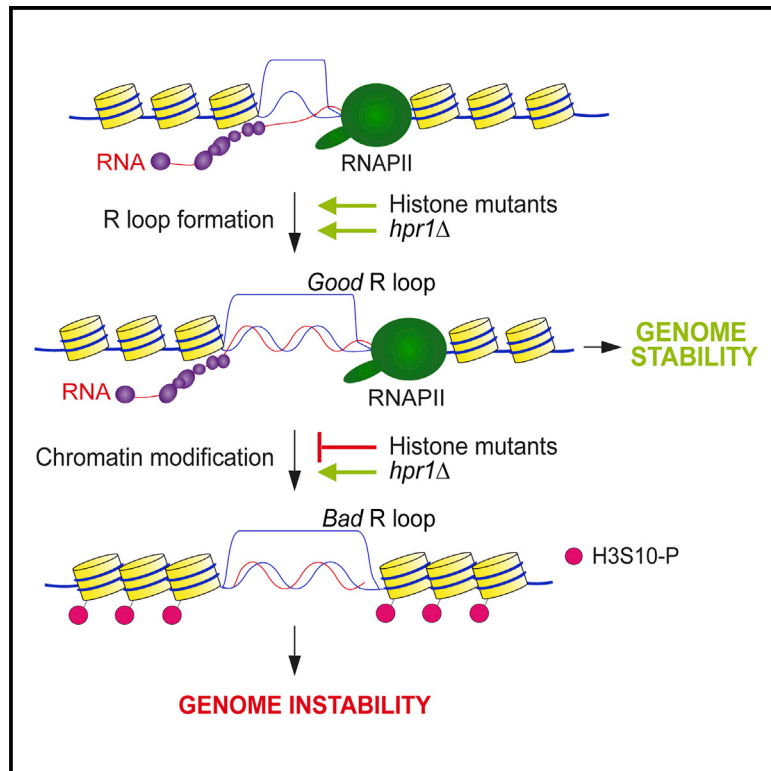# Molecular Cell

Histone Mutants Separate R Loop Formation from Genome Instability Induction

Graphical Abstract

Authors

Desiré García-Pichardo,
Juan C. Cañas, María L. García-Rubio,
Belén Gómez-González,
Ana G. Rondón, Andrés Aguilera

Correspondence

aguilo@us.es

In Brief

R loops can cause genome instability. However, García-Pichardo et al. identify histone H3/H4 mutants that demonstrate that R loops alone are not enough. Instead, further chromatin modifications, including H3 serine-10 phosphorylation, are necessary. They conclude that once R loops form, an additional chromatin modification step is required for genome instability.

Highlights

- Histones represent a first barrier to R loop formation

- R loops per se do not cause genetic instability

- H3 serine-10 phosphorylation is required for R loop-mediated genetic instability

- Histone mutants unable to phosphorylate H3S10 suppress *hpr1* genome instability

CrossMark

CellPress

Article

Histone Mutants Separate R Loop Formation from Genome Instability Induction

Desiré García-Pichardo,[1] Juan C. Cañas,[1] María L. García-Rubio,[1] Belén Gómez-González,[1] Ana G. Rondón,[1] and Andrés Aguilera[1,2,*]

[1]Centro Andaluz de Biología Molecular y Medicina Regenerativa-CABIMER, Universidad de Sevilla-CSIC-Universidad Pablo de Olavide, Seville 41092, Spain
[2]Lead Contact
*Correspondence: aguilo@us.es
http://dx.doi.org/10.1016/j.molcel.2017.05.014

SUMMARY

R loops have positive physiological roles, but they can also be deleterious by causing genome instability, and the mechanisms for this are unknown. Here we identified yeast histone H3 and H4 mutations that facilitate R loops but do not cause instability. R loops containing single-stranded DNA (ssDNA), versus RNA-DNA hybrids alone, were demonstrated using ssDNA-specific human AID and bisulfite. Notably, they are similar size regardless of whether or not they induce genome instability. Contrary to mutants causing R loop-mediated instability, these histone mutants do not accumulate H3 serine-10 phosphate (H3S10-P). We propose a two-step mechanism in which, first, an altered chromatin facilitates R loops, and second, chromatin is modified, including H3S10-P, as a requisite for compromising genome integrity. Consistently, these histone mutations suppress the high H3S10 phosphorylation and genomic instability of *hpr1* and *sen1* mutants. Therefore, contrary to what was previously believed, R loops do not cause genome instability by themselves.

INTRODUCTION

Genome instability is a major threat to cell survival, along with being the origin of multiple diseases including cancer. Metabolic processes occurring on the DNA are important sources of genome instability; failures in DNA replication or the DNA damage response (DDR) are the most common cause (Aguilera and García-Muse, 2013). Transcription is an important source of replication stalling and impairment, either directly by becoming an obstacle to the progression of replication forks or indirectly by generating harmful transcriptional byproducts such as R loops (Castellano-Pozo et al., 2013; Gan et al., 2011; Wellinger et al., 2006).

R loops, RNA-DNA hybrids and the displaced single-stranded DNA (ssDNA), are formed in *cis* by the nascent RNA threading back to hybridize with the template DNA strand. Although

R loops are intermediate structures in important biological processes like immunoglobulin class switching or mitochondrial replication, their uncontrolled formation can be a significant cause of genome instability. Consequently, multiple cellular mechanisms operate to prevent the deleterious effects of R loops (Santos-Pereira and Aguilera, 2015). RNA binding and processing factors, like THO, ASF/SF2, or AQR, and topoisomerases have key roles in preventing R loop formation (Domínguez-Sánchez et al., 2011; El Hage et al., 2010; Huertas and Aguilera, 2003; Li and Manley, 2005; Sollier et al., 2014; Yang et al., 2014); RNase H, Sen1/SETX, DDX19, and DDX23 in eliminating them (Hodroj et al., 2017; Mischo et al., 2011; Skourti-Stathaki et al., 2014; Sridhara et al., 2017); and DNA repair mechanisms such as BRCA and Fanconi anemia in precluding their DNA damaging effects (Bhatia et al., 2014; García-Rubio et al., 2015; Hatchi et al., 2015; Schwab et al., 2015). Elimination of any one of these activities causes R loop accumulation and genetic instability (Santos-Pereira and Aguilera, 2015).

Chromatin may constitute a barrier to many processes occurring on the DNA, including transcription, replication, and DNA repair. Post-translational modification of histones, mainly at the unfolded N-terminal tails but also at the core, influences nucleosome dynamics by recruiting chromatin remodelers, histone chaperones, and specific factors that facilitate or restrict access to DNA (Tessarz and Kouzarides, 2014). Certainly, it is possible that chromatin might control R loop formation or stability, among many other processes; however, this has not been directly tested as yet. In this sense, it has been shown that the histone chaperone complex FACT is involved in precluding R loop accumulation (Herrera-Moyano et al., 2014), but whether histones themselves have a protective role over the genome preventing harmful R loop buildup is still unknown.

To investigate this possibility, we screened a *Saccharomyces cerevisiae* library of histone H3 and H4 point mutants to identify mutations favoring the formation of R loops. Importantly, the R loop accumulating mutants identified, as confirmed by genetic and molecular assays, do not lead to genome instability by themselves, but only when human activation-induced cytidine deaminase (AID) is ectopically overexpressed. This is not due to a different size of the RNA-DNA hybrid, which is similar in wild-type and R loop-accumulating strains, whether or not it causes hyper-recombination. Instead, the lack of R loop-associated genome instability correlates with the inability to support histone H3 serine-10 phosphorylation. Notably, the
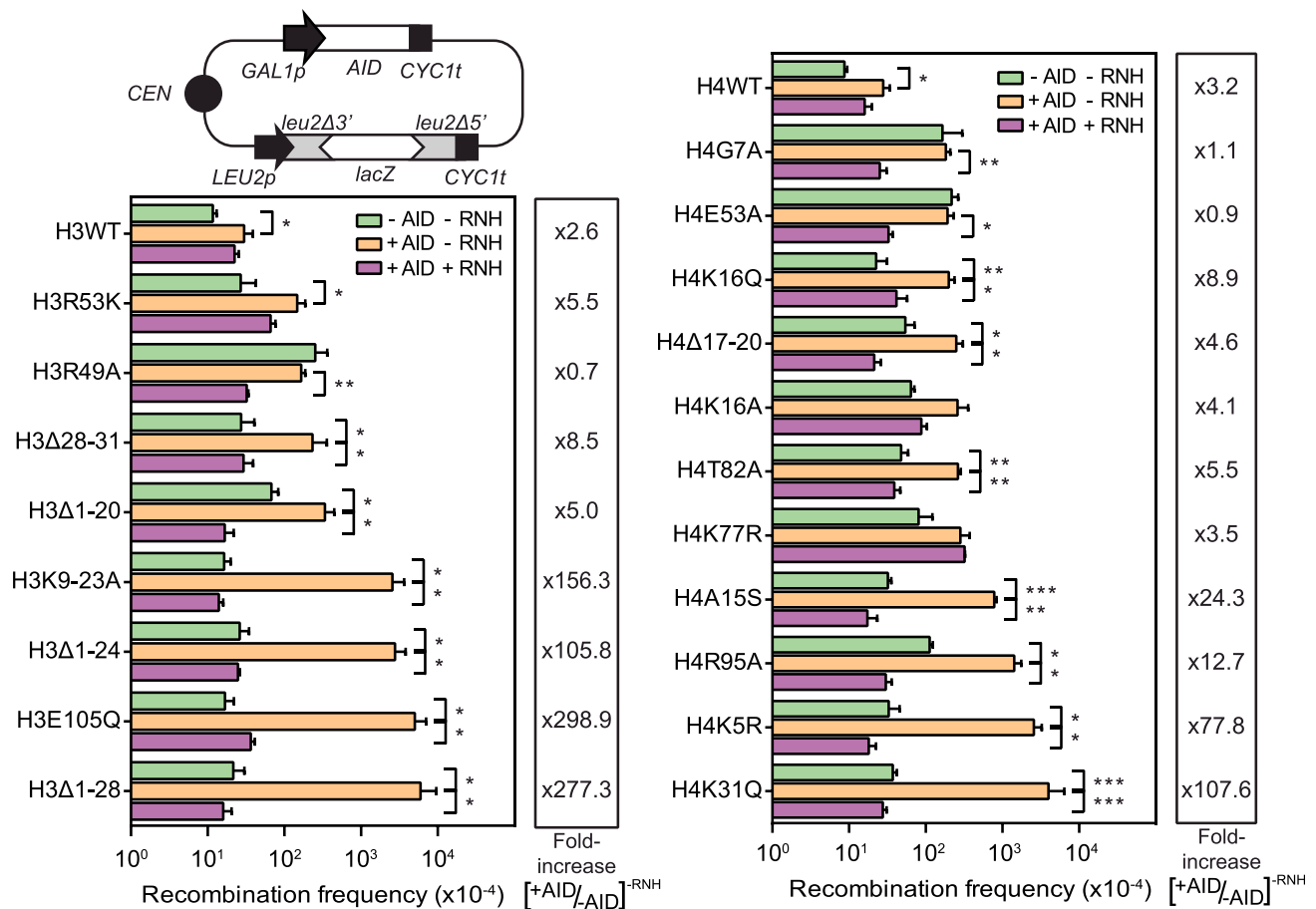
Figure 1. Mutations in Histones H3 and H4 Increase Recombination in an AID-Dependent and RNase H1-Sensitive Manner

Schematic representation of pLZGAID plasmid used in the screening. Recombination frequencies in wild-type (H3WT or H4WT) and mutant strains carrying point mutations or deletions in H3 (R53K, R49A, Δ28-31, Δ1-20, K9-23A, Δ1-24, E105Q, and Δ1-28) or H4 (G7A, E53A, K16Q, Δ17-20, K16A, T82A, K77R, A15S, R95A, K5R, and K31Q) selected as positive candidates in the screening with (+) or without (−) AID or RNase H1 (RNH) overexpression (n = 3). Means and SEM are plotted in all panels. *p ≤ 0.05; **p ≤ 0.01; ***p ≤ 0.001 (two-tailed Student's t test). See also Figure S1.

hyper-recombination phenotype of *hpr1* and *sen1* mutants is suppressed by these histone mutations. Our study shows, therefore, that the R loop itself does not compromise genome integrity unless a subsequent step of chromatin modification, linked to histone H3 serine-10 phosphorylation in this case, occurs.

RESULTS

Identification of Histone H3 and H4 Mutations that Facilitate R Loop Formation

We screened the Non-Essential Histone H3 and H4 Mutant Collection of *Saccharomyces cerevisiae* (Dai et al., 2008) for histone mutations that enhanced R loop accumulation. We used human AID as a tool to detect R loops because AID targets cytidines present in ssDNA inducing DNA damage (Chaudhuri et al., 2003; Sohail et al., 2003). We have previously shown that AID expression in R loop-accumulating yeast mutants increases recombination and C-to-T transitions at the ssDNA, consistent with its preferential action on the ssDNA displaced by the RNA in the R loop (Gómez-González and Aguilera, 2007; Mischo

et al., 2011). Therefore, we cloned AID under the *GAL1p* inducible promoter in a centromeric plasmid containing the *leu2Δ3′::lacZ::leu2Δ5′* direct-repeat recombination system *L-lacZ* (Figure 1). The new plasmid, pLZGAID, was used to transform the Non-Essential Histone H3 and H4 Mutant Collection. After the induction of AID expression by growth in galactose-containing media, AID-mediated hyper-recombinant mutants were screened in selective media lacking leucine to detect Leu+ recombinants (Figure S1A). Recombination frequencies were assayed in the selected candidates with or without AID expression and with or without RNase H1 overexpression to determine the influence of R loops. RNase H1 specifically degrades the RNA moiety of an RNA-DNA hybrid, eliminating the R loops (Crouch et al., 2001). Eight histone H3 mutants and eleven histone H4 mutants increased recombination ≥ five times over wild-type levels in the presence of AID, but only in six of the H3 and seven of the H4 mutants was recombination significantly AID dependent (increased in the presence of AID) and RNase H1 sensitive (suppressed by RNH1 overexpression), implying that it was R loop dependent (Figure 1). We confirmed that this increase in

recombination was not due to the change of the carbon source, from glucose to galactose, but to AID expression (Figure S1B). Importantly, these histone mutants are not hyper-recombinant per se, in contrast to previously identified R loop-accumulating mutants such as *hpr1Δ* or *sen1-1*, where AID overexpression enhances a preexisting hyper-recombination phenotype (Gómez-González and Aguilera, 2007; Mischo et al., 2011).

The histone mutations causing AID-dependent hyper-recombination were preferentially located in the N-terminal H3 and H4 histone tails. The H3 mutants contained mutations located mainly in the first 28 residues. Deletion of these residues (Δ1-28 or Δ1-24) or substitutions of the N-terminal tail lysines 9, 14, 18, and 23 to alanines (K9-23A) increased recombination more than 105 times, exclusively under AID overexpression (Figure 1). The only H3 mutant with an AID-dependent hyper-recombinant phenotype not located in the N-terminal tail was the replacement of the glutamic acid 105 present in the globular domain by glutamine (E105Q). Mutants in H4 also tended to accumulate in the N-terminal tail (Δ17-20, K5R, A15S, and K16Q). Lysine 31 to glutamine (K31Q) conferred the strongest hyper-recombination with a 108-fold increase compared to the levels in the absence of AID (Figure 1). Therefore, from now on we pursued our analysis with the N-terminal tail mutants H3Δ1-28 and H3K9-23A from histone H3 and H4K31Q from histone H4 as the representative mutants that cause genetic instability only when AID is expressed. Importantly, we confirmed by chromatin immunoprecipitation (ChIP) analysis that the differences in AID-mediated instability observed between the wild-type and these histone mutants are not caused by changes in the ability of AID to be recruited to chromatin (Figure S1C).

Histone H3Δ1-28, H3K9-23A, and H4K31Q Mutants Only Induce Different Types of Genome Instability in an AID-Dependent Manner

To further analyze the AID-dependent hyper-recombination observed in the selected histone mutants, we first confirmed it in a chromosomal context using a recombination system based on two mutated copies of the *HIS3* gene placed in a direct-repeat orientation in the right arm of chromosome XV (Figure 2A) (Aguilera and Klein, 1988). Recombination was measured as the frequency of His+ colonies with or without AID and RNase H1 overexpression. The results confirmed the data obtained with the original pLZGAID plasmid used for the screening: a significant increase in recombination uniquely observed in the presence of AID (from 67- to 94-fold) that is RNase H sensitive (Figure 2A). This result shows that the AID-dependent genetic instability phenotype occurs in both chromosomal and plasmid systems.

To globally measure recombinogenic DNA damage in the cell, we used a version of the Rad52 recombination factor fused to the yellow fluorescent protein (YFP) (Lisby et al., 2001). A significant increase in Rad52 foci was observed upon AID expression (40%–80% above the levels in the absence of AID), and it was fully suppressed by RNase H1 overexpression (Figure 2B). Consistent with the AID-dependent hyper-recombination observed in the plasmid and chromosomal systems, H3Δ1-28, H3K9-23A, and the H4K31Q histone mutants did not increase Rad52 foci unless AID was expressed (Figure 2B). These results indicate that the action of AID on the ssDNA of R loops is not

limited to the recombination systems used but is general throughout the genome.

The results on Rad52 foci and recombination frequencies suggest that H3Δ1-28, H3K9-23A, and H4K31Q mutants do not cause genetic instability by themselves. To confirm this, we performed a broader analysis of genetic instability phenotypes that included loss of heterozygosity (LOH), chromosome loss, plasmid loss, mutagenicity, and DNA damage checkpoint activation (Figures 2C–2E and S2A). The three histone mutants show LOH levels, as measured at the *MAT* locus in homozygous diploid strains, similar or slightly lower than those of wild-type cells and significantly lower than those of the *hpr1Δ* mutant, a THO mutant used as a positive control (Figure 2C), a result that can be extended to chromosome III loss, provided that 25% (15 out of 59 independent clones) of the LOH events at the *MAT* locus were due to chromosome loss, as determined by qPCR (see STAR Methods). For a more precise analysis, we analyzed the frequency of loss of the centromeric plasmid pRS414, which allowed us to determine whether any possible phenotype could be suppressed by RNase H1. As expected from the chromosome loss results, the basal levels of plasmid loss of the mutants were slightly lower or similar to wild-type cells. Although only statistically significant in H3K9-23A, there was a consistent increase in plasmid loss induced by AID expression (1.8- to 2.5-fold increase) in the two H3 mutants that was fully suppressed by RNase H1 (Figure 2D).

Spontaneous mutation levels, another measure of genome instability, were determined for the chromosomal *CYH2* locus as the frequency of cyclohexymide-resistant colonies. The histone mutants showed spontaneous mutation levels similar to wild-type cells or even lower, except H4K31Q. Importantly, mutation levels were significantly increased after AID expression (2- to 3-fold above the levels in the absence of AID) (Figure 2E). These phenotypes indicate that the DNA damage is induced by AID. However, such damage neither causes a detectable S-phase checkpoint activation, as determined by Rad53 phosphorylation (Figure S2A), nor affects cell-cycle progression or recombination even in the presence of the dNTP-depleting drug HU (Figures S2B and S3A). Consistently, these mutants are not sensitive to genotoxic agents like MMS, HU, or UV light (Figure S3B), with the exception of H3Δ1-28, as previously reported (Dai et al., 2008). Taken together, these observations suggest that the relevant characteristic of these histone mutants is not to induce DNA damage but to facilitate the formation of the AID substrate, ssDNA, consistent with the formation of R loops, and as shown by the suppression of the AID-dependent phenotypes by RNase H1 overexpression.

Histone H3Δ1-28, H3K9-23A, and H4K31Q Mutants Accumulate R Loops

Once shown by different genetic assays that R loops should be accumulating in the selected histone mutants, we decided to directly detect RNA-DNA hybrids. For this, we performed DNA-RNA immunoprecipitation (DRIP) analysis using the S9.6 antibody in the *GCN4* and *TPD3* genes, previously described to form RNA-DNA hybrids (Castellano-Pozo et al., 2013; Chan et al., 2014; Herrera-Moyano et al., 2014), and in the long gene *YLR454w* fused to the *GAL1* promoter. The S9.6 signal in H3Δ1-28, H3K9-23A, and
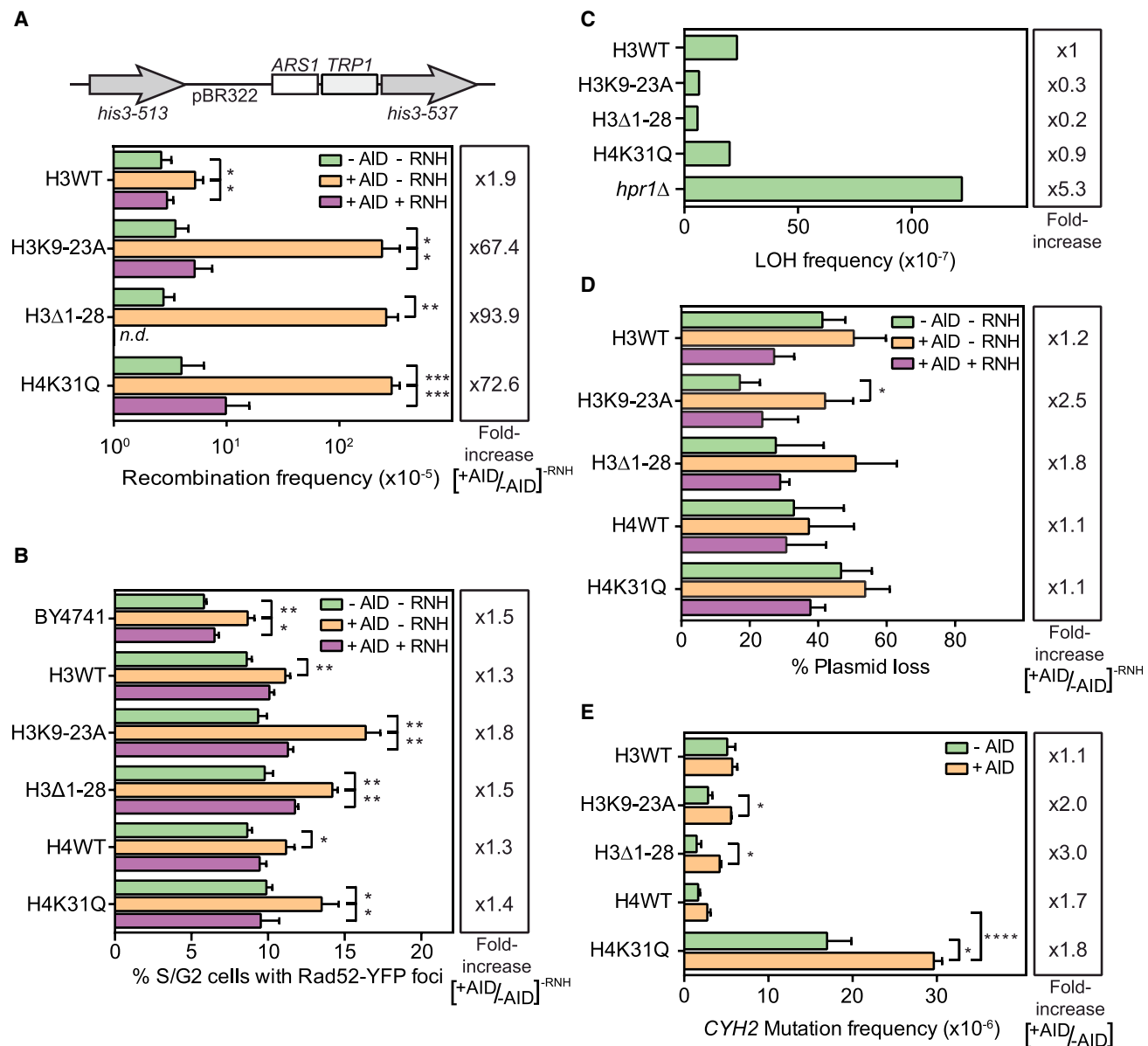
Figure 2. Mutations in the H3 N-Terminal Tail and H4K31 Only Cause Genetic Instability in an AID-Dependent Manner

(A) Schematic representation of the chromosomal *his3*-based direct-repeat recombination system. Recombination frequencies with (+) or without (−) AID or RNase H1 (RNH) overexpression (n = 3).

(B) Percentage of Rad52-YFP foci formation with (+) or without (−) AID or RNH overexpression (n = 3).

(C) Frequency of loss of heterozygosity (LOH) in the *MAT* locus at chromosome III (n = 6).

(D) Percentage of pRS414 centromeric plasmid loss with (+) or without (−) AID or RNase H1 (RNH) overexpression (n = 4).

(E) Frequency of spontaneous *CYH2* mutation with (+) or without (−) AID overexpression (n = 4).

Experiments from (A)–(E) were performed in the H3WT, H3K9-23A, H3Δ1-28, H4WT, and H4K31Q mutants.

Means and SEM are plotted in (A), (B), (D), and (E), and the median is plotted in (C). *$p \leq 0.05$; **$p \leq 0.01$; ***$p \leq 0.001$; ****$p \leq 0.0001$ (two-tailed Student's t test). See also Figures S2 and S3. n.d., not detected.

H4K31Q mutants was significantly higher than in the isogenic wild-type strains and, as expected, disappeared after in vitro RNase H treatment. Importantly, this occurred in asynchronous (Figures 3A and S4), G1-, and S-synchronized cell cultures (Figure 3B), ruling out that this accumulation of RNA-DNA hybrids was the result of a replication intermediate.

To establish a direct correlation between the AID-dependent increase in recombination observed in H3Δ1-28, H3K9-23A, and H4K31Q mutants and the R loop accumulation, we performed DRIP in the chromosomal *his3* direct-repeat system where we saw the hyper-recombination phenotype (Figure 2A). We observed a significant accumulation of RNA-DNA hybrids
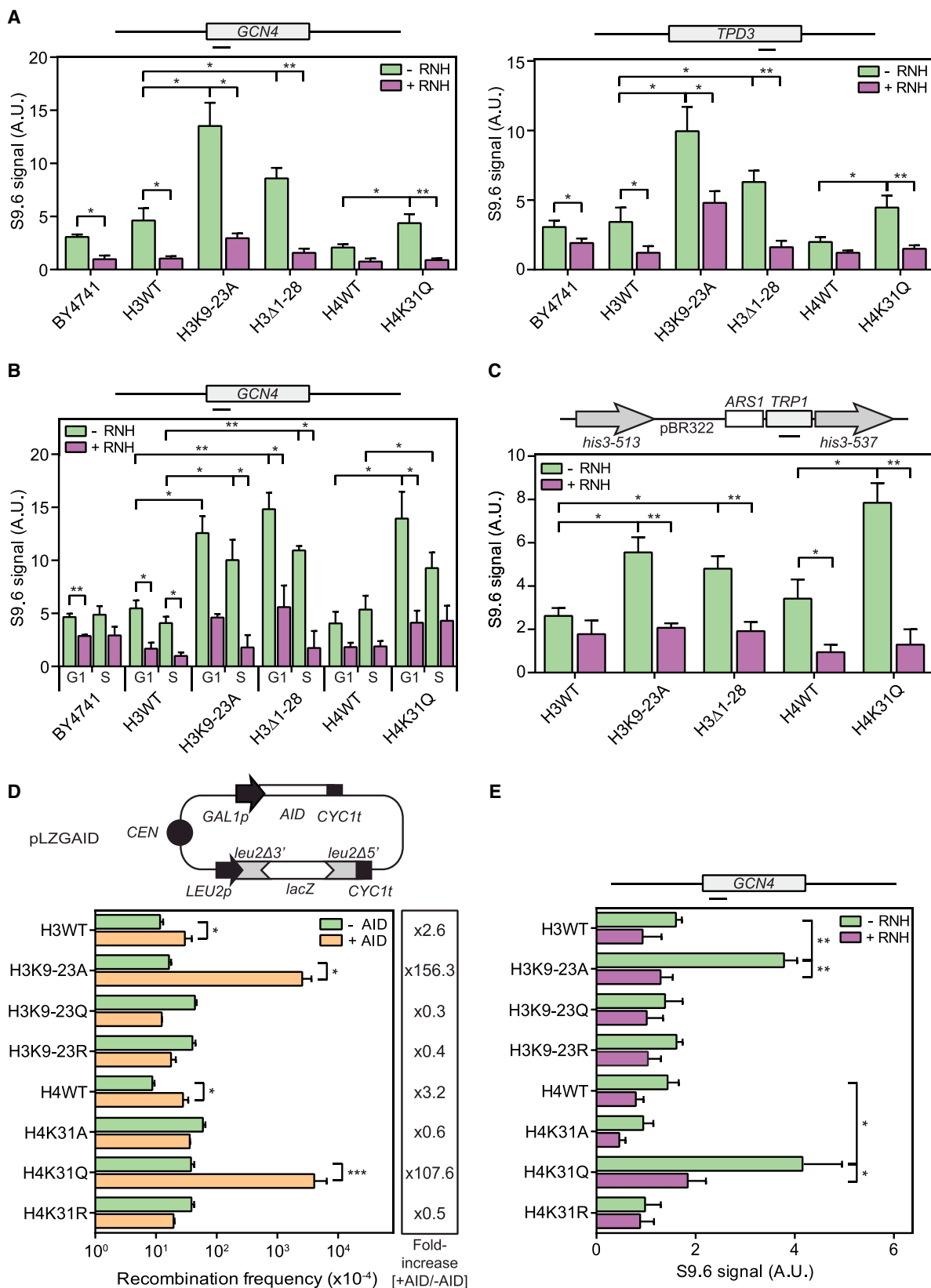
(legend on next page)

in the transcribed *TRP1* gene located between the *his3* repeats in the three histone mutants analyzed (Figure 3C). Therefore, these mutants indeed facilitate RNA-DNA hybrid formation, although such hybrids do not activate the DDR and do not confer a detectable genome instability phenotype by themselves. The fact that AID stimulates recombination in these mutants, as also previously shown for *hpr1Δ* mutants (Gómez-González and Aguilera 2007), implies that those RNA-DNA hybrids are accompanied by the ssDNA susceptible to being modified by AID. Therefore, such histone mutants indeed accumulate full R loop structures containing the RNA-DNA hybrid and the displaced ssDNA.

Since lysines were systematically replaced by alanines, arginines, and glutamines in the histone mutant collection that we screened, we wanted to test if other mutations in histone H3K9-23 and H4K31 enhanced R loops. Notably, the AID-dependent increase in recombination was not observed in the H3K9-23Q, H3K9-23R, H4K31A, and H4K31R mutants, indicating that it was specific to H3K9-23A and H4K31Q mutants (Figure 3D). Consistently, DRIP analysis in the *GCN4* gene confirmed that H3K9-23A and H4K31Q mutations increased RNA-DNA hybrids, whereas the other four did not (Figure 3E). Therefore, changes of H3K9-23 and H4K31 to A and Q, respectively, and not to other amino acids, make chromatin R loop prone.

R Loops Are Similar in Size Regardless of Whether or Not They Induce Genome Instability

One possible explanation of why the R loops observed in the selected histone mutants do not induce genome instability by themselves is that they are shorter than those that compromise genome integrity like the R loops observed in *hpr1Δ* mutants. Therefore, we determined R loop length by bisulfite mutagenesis and subsequent amplification and sequencing of single molecules (Yu et al., 2003) in wild-type, histone mutants, and *hpr1Δ*. Due to the low frequency of R loops, an enrichment method with one converted primer (C; which anticipates C-to-U changes provoked by bisulfite) and one conventional primer (N; native) was used for the PCR to preferentially amplify the DNA molecules containing RNA-DNA hybrids, following previously reported strategies (Figure 4A) (Yu et al., 2003). When the converted primer was designed to align the non-transcribed strand (NTS), which is predicted to be single stranded in an R loop (Figure 4A), PCR amplification was only detected reproducibly at the 3′ end of the gene (N1C3) (Figure 4B). In agreement with the transcribed strand (TS) being protected by the paired RNA, the complementary reaction with a converted primer aligning to the TS did not lead to any PCR amplification (C4N5) (Figure 4B), indicating that these signals were indeed due to R loop formation and not to transient opening of the DNA. Notably, DNA

sequencing confirmed the expected C-to-T changes and revealed that these regions were similar in size, with a mean of 164 bp in the wild-type, 153 bp in *hpr1Δ*, and ranging from 125 to 172 bp in the different histone mutants (Figure 4C). The results confirm that full R loops, composed of the RNA-DNA hybrid and the displaced ssDNA, are formed in histone mutants as well as in wild-type and *hpr1Δ* strains. However, the R loops in the histone mutants selected do not differ in size from those of either wild-type or *hpr1Δ* hyper-recombinant mutants. Therefore, differences in R loop length do not explain why some cause genome instability, but not others.

Chromatin Plays a Key Role in Preventing R Loop Formation

Since changes in chromatin structure could alter transcription rates and higher mRNA production might correlate with enhanced R loop formation (Chan et al., 2014; Wahba et al., 2016), we measured transcript levels by northern analysis and by RNA polymerase II (RNAPII) ChIP. The level of *GCN4* mRNA and RNAPII occupancy at either *GCN4* or *TPD3* did not vary substantially in the mutants (Figures S5A and 5A), indicating that transcription was not significantly affected and cannot, therefore, explain the high levels of R loops. Alternatively, hybrids could be favored if the mutant chromatin makes the DNA more accessible. Indeed, truncation of the H3 N-terminal 28 residues alters DNA-histone interactions, reducing the stability of the nucleosome (Ferreira et al., 2007). Furthermore, the variation in charge introduced with K31Q mutation disrupts the interaction between K31 side chain and DNA (Iwasaki et al., 2011), which might facilitate RNA hybridization. We therefore determined whether nucleosome occupancy was altered. H3Δ1-28 and H3K9-23A mutants significantly reduced histone H3 presence in chromatin in the constitutive genes *GCN4* and *TPD3* and in the inducible *GAL1* gene and *GAL1p::YLR454w* construct (Figures 5B and S5B). In the H4K31Q mutant, histone H3 occupancy tends to decrease, but this was only seen in some of the genes analyzed (Figures 5B and S5B). The global level of histone H3 was not altered in the three histone mutants studied (Figure S5C). Interestingly, H3 occupancy in the H3K9-23Q, H3K9-23R, H4K31A, and H4K31R mutants that did not show R loop-dependent hyper-recombination or R loop accumulation was similar to the H3K9-23A and H4K31Q mutants, consistent with the conclusion that the detectable changes in histone occupancy are not determinant of R loop formation (Figure S5D).

Finally, given that DNA wrapping around a nucleosome introduces a single negative supercoil in circular DNA molecules, we tried to infer changes in chromatin by analyzing topoisomer distribution in a circular plasmid. The results showed a slight

---

Figure 3. Mutations in the H3 N-Terminal Tail and H4K31 Cause RNA-DNA Hybrid Accumulation

(A) DRIP with the S9.6 antibody in BY4741, H3WT, H3K9-23A, H3Δ1-28, H4WT, and H4K31Q strains in asynchronous cultures treated (+) or not (−) in vitro with RNase H in the *GCN4* and *TPD3* genes (n ≥ 3).

(B) As in (A) in G1- or S-arrested cells in *GCN4* gene (n = 3).

(C) As in (A) in the *his3*-based direct-repeat recombination system.

(D) Recombination frequencies in wild-type (H3WT or H4WT) and point mutations in either H3K9, K14, K18, and K23 or H4K31 to alanine (A), glutamine (Q), or arginine (R) with (+) or without (−) AID, using the pLZGAID plasmid (n = 3).

(E) DRIP with the S9.6 antibody in H3WT, H3K9-23A, H3K9-23Q, H3K9-23R, H4WT, H4K31A, H4K31Q, and H4K31R strains in asynchronous cultures treated (+) or not (−) in vitro with RNase H in the *GCN4* gene (n = 3).

Means and SEM are plotted in all panels. *p ≤ 0.05; **p ≤ 0.01; ***p ≤ 0.001 (two-tailed Student's t test). See also Figure S4.

A

B

C
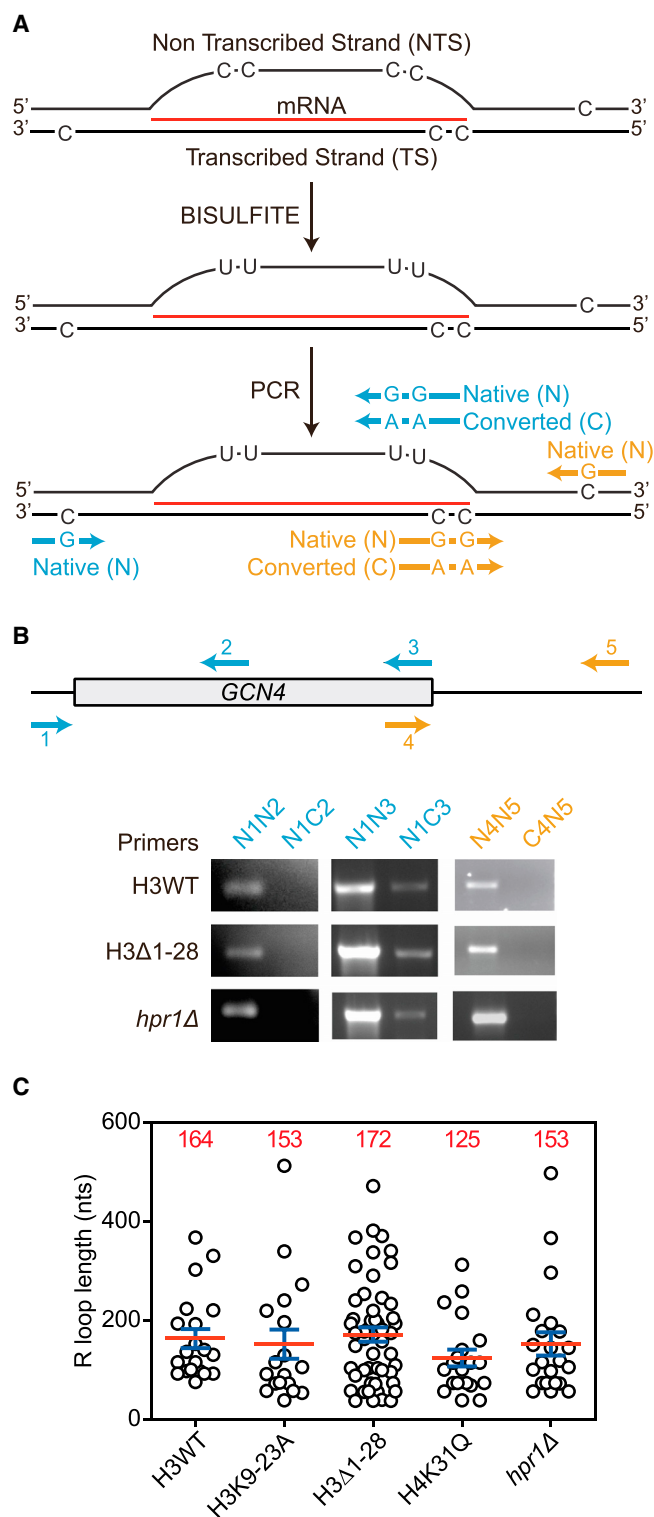
Figure 4. The R Loop Length Is Not Different in Mutations in the H3 N-Terminal Tail, H4K31, and hpr1Δ

(A) Diagram of the bisulfite modification assay for detection of R loops.

(B) Detection of R loops by PCR in the different depicted regions of the *GCN4* gene in H3WT, H3Δ1-28, and *hpr1Δ* (YDR138W) strains with the indicated native (N) or converted (C) forward and reverse primers.

positive supercoiled shift in the H3Δ1-28, H3K9-23A, and H4K31Q mutants that was clearer in the 2D gels under non-transcribed conditions (Figures 5C, S6A, and S6B). The observations suggest that the histone mutants may affect nucleosome-DNA interaction. However, further analysis of their chromatin structure is needed to determine with precision the nature of the chromatin changes that make DNA more R loop prone. This is important for specific mutants like H3Δ1-28, in which a significantly low nucleosome occupancy was apparent in some of the genes tested, such as the *GAL1::YLR454w*.

Histone H3 Serine-10 Phosphorylation Is Required for the R Loop-Mediated Genome Instability Observed in Hyper-recombinant Mutants

We have previously shown that R loops trigger high levels of histone H3S10-P in hyper-recombinant *hpr1Δ* cells, particularly in G1, the cell-cycle phase in which H3S10-P levels are at their lowest in wild-type cells (Castellano-Pozo et al., 2013). Since this residue was missing in the H3Δ1-28 mutant, we reasoned that an inability to undergo high levels of H3S10-P could explain the differences in genomic instability observed. We found that the H3K9-23A and H4K31Q mutants synchronized in G1 did not undergo high levels of histone H3S10-P (Figure 6A). To assess whether lack of H3S10-P was generally associated with R loops incapable of inducing instability, we extended the analysis to other mutants selected in the screening that showed an AID-dependent RNase H-sensitive hyper-recombination: H3Δ28-31, H3E105Q, H4K5R, H4A15S, H4T82A, and H4R95A. Interestingly, the overall levels of H3S10-P in G1 cells were low in all these mutants and similar to wild-type levels (Figure 6B). A closer look at the regions enriched in R loops revealed that H3S10-P did not accumulate in either the pLZGAID system where AID-dependent hyper-recombination was observed or in the *GCN4* and *TPD3* genes where RNA-DNA hybrids were detected in H3K9-23A and H4K31Q mutants (Figure 6C). Therefore, R loops that do not cause genome instability per se do not increase the levels of H3S10-P.

We next wondered whether H3S10-P was necessary for R loop-associated instability in other mutants. If so, mutating the N-terminal tail residues H3Δ1-28, H3K9-23, or H4K31 should suppress R loop-mediated genome instability. To test this hypothesis, we made double mutants of H3Δ1-28, H3K9-23A, or H4K31Q with *hpr1Δ*, an R loop-dependent hyper-recombinant mutant (Huertas and Aguilera, 2003). Effectively, in the double mutants, the H3S10-P signal decreased to wild-type levels (Figure 6D). Consistent with a requirement of H3S10-P for R loop-mediated instability, we found that the hyper-recombination phenotypes of R loop-accumulating *hpr1Δ* and *sen1-1* mutants were also suppressed by the H3K9-23A, H3Δ1-28, or H4K31Q mutations (Figures 7A and 7B). To confirm the suppression of genome instability, we extended the analysis to Rad52 foci accumulation, a marker of DNA damage in the cell. Precluding H3S10 phosphorylation also diminished Rad52 foci in *hpr1Δ* or *sen1-1* mutants (Figures 7C and 7D). Taken together, these observations

(C) Distribution of the R loop length in H3WT, H3K9-23A, H3Δ1-28, H4K31Q, and *hpr1Δ* (YDR138W) strains detected by bisulfite modification assay in the *GCN4* gene. Mean and SEM of 18–35 clones are shown.

A

B

C
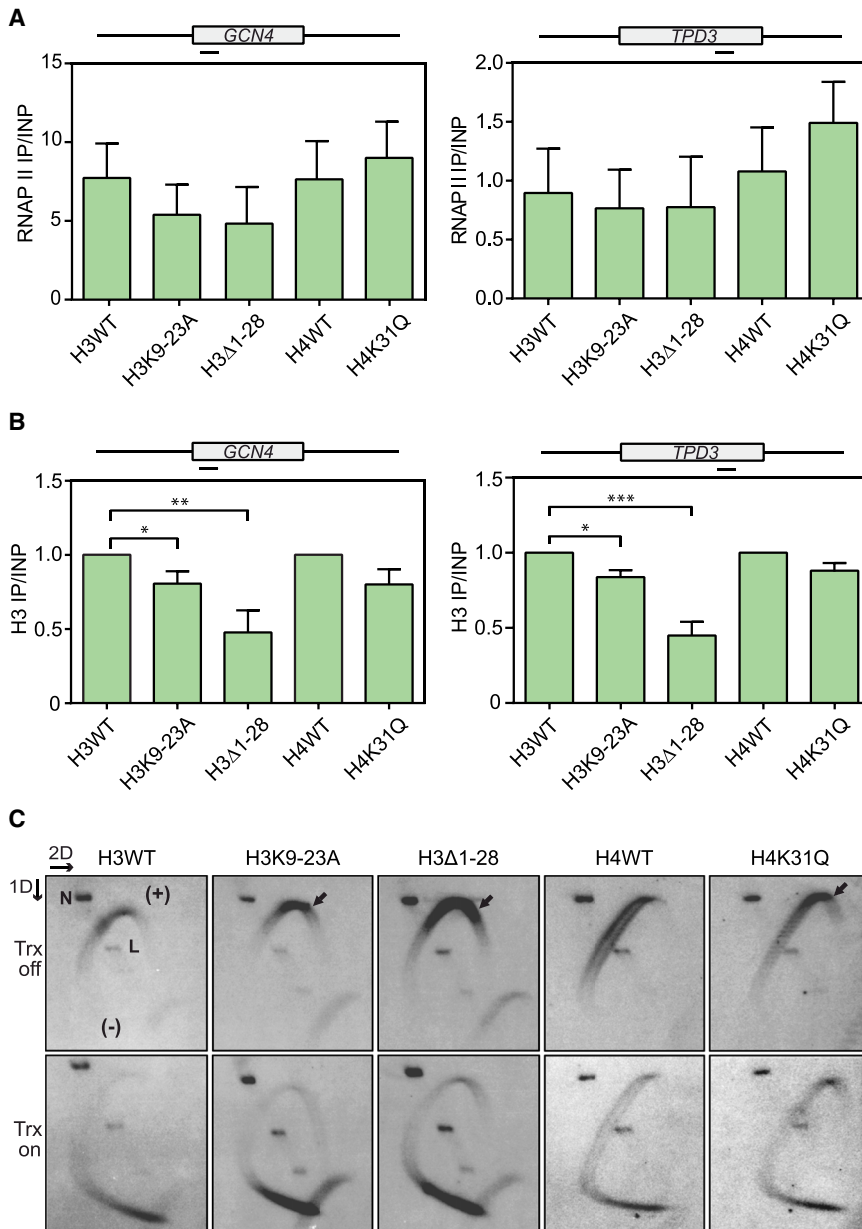
Figure 5. Nucleosome Density Is Decreased in H3 N-Terminal Tail Mutants

(A) ChIP analysis of RNAPII occupancy in H3WT, H3K9-23A, H3Δ1-28, H4WT, and H4K31Q strains in the *GCN4* and *TPD3* genes (n = 3).

(B) ChIP analysis using H3 antibody in the constitutive *GCN4* and *TPD3* genes (n ≥ 4). Means and SEM are plotted in both panels. *p ≤ 0.05; **p ≤ 0.01; ***p ≤ 0.001 (two-tailed Student's t test).

(C) Plasmid pRSGALlacZ topoisomer distribution in 2D chloroquine gels under active (ON) or repressed (OFF) conditions. Nicked (N) and linear (L) forms are indicated. Black arrows indicate the DNA migration shift caused by the change in supercoiling.

See also Figures S5 and S6.

AID-induced recombination and bisulfite mutagenesis (Figures 3 and 4). This implies that not only the formation of a properly assembled mRNP during transcription (Aguilera, 2005) but also the chromatin structure plays a key role in preventing R loops. Importantly, in contrast to all R loop-accumulating yeast mutants reported until now, such as *hpr1*, *rnh1*, *sen1*, *npl3*, and *sin3*, and mRNA 3′ end processing factors (Huertas and Aguilera, 2003; Mischo et al., 2011; Santos-Pereira et al., 2013; Stirling et al., 2012; Wahba et al., 2011), genetic instability, as determined by Rad52 foci and hyper-recombination, is not observed in these histone mutants unless AID is overexpressed (Figures 1 and 2). Therefore, we report here that R loops alone are not sufficient to compromise genome integrity by themselves.
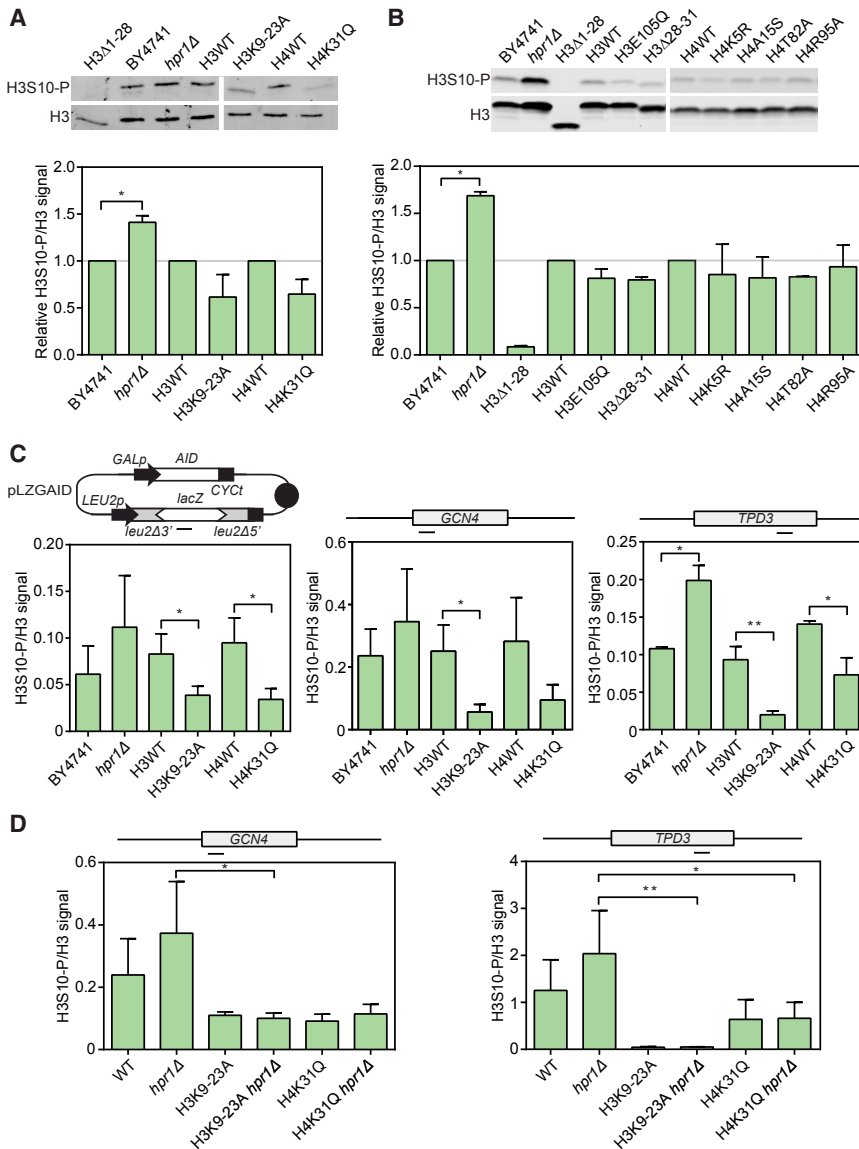
The specific mutations in H3 N-terminal tail and H4K31 analyzed here increase R loop levels in the cell, without enhancing transcription (Figures 5 and S5). Importantly, only the changes of H3K9-23 to A, but not to Q or R, and

indicate that R loop-mediated genome instability is not caused by the R loop itself, but by subsequent and additional events altering chromatin, such as histone H3 serine-10 phosphorylation.

DISCUSSION

AID induces recombination in yeast strains accumulating R loops, such as *hpr1Δ* (Gómez-González and Aguilera, 2007), and we used this property to identify a number of histone H3 and H4 mutants that increase instability in an AID-dependent and RNase H-sensitive manner. Molecular analysis of these mutant shows that they do indeed accumulate R loops containing RNA-DNA hybrids plus the displaced ssDNAs as shown by

of H4K31 to Q, but not to A or R, promote R loops (Figure 3), implying a unique impact of H3K9-23A and H4K31Q mutations on chromatin structure and dynamics to favor R loop formation. Acetylation of H3 lysines 9, 14, 18, and 23 is the only modification reported in these residues in *S. cerevisiae* (Smolle and Workman, 2013). H3K9 is also methylated in other eukaryotes, but not in the budding yeast. In histone H4, no modification has been reported for the lysine 31 in *S. cerevisiae*, but it can be methylated, acetylated, or ubiquitylated in mouse and humans (Garcia et al., 2007; Kim et al., 2013). Apart from blocking possible post-translational modifications, mutations in the lysines of the histone tails could alter DNA-nucleosome interaction or destabilize the nucleosome

A

B

C

D

Figure 6. Mutations in the H3 N-Terminal Tail and H4K31 Suppress H3 Serine-10 Phosphorylation in the R Loop-Accumulating *hpr1Δ* Mutant

(A) Immunoblot showing H3S10-P of cell extracts from *hpr1Δ* (YDR138W), H3Δ1-28, H3K9-23, and H4K31Q mutants arrested in G1. Signals normalized to H3 are plotted (n = 3). Only the increased values were subjected to statistical analysis of significance.

(B) As in (A) in hpr1δ (YDR138W), H3δ1-28, H3E105Q, H3Δ28-31, H4K5R, H4A15S, H4T82A, and H4R95A mutants.

(C) ChIP analysis of H3S10-P normalized to H3 in strains arrested in G1 (n ≥ 3) in the *lacZ* gene of the pLZGAID plasmid and in the endogenous *GCN4* and *TPD3* genes.

(D) As in (C) in simple and double *hpr1* and histone mutant strains arrested in G1 in the *GCN4* and *TPD3* genes (n = 4).

Means and SEM are plotted in all panels. *p ≤ 0.05; **p ≤ 0.01 (Mann-Whitney test in A and B; two-tailed Student's t test in C and D).
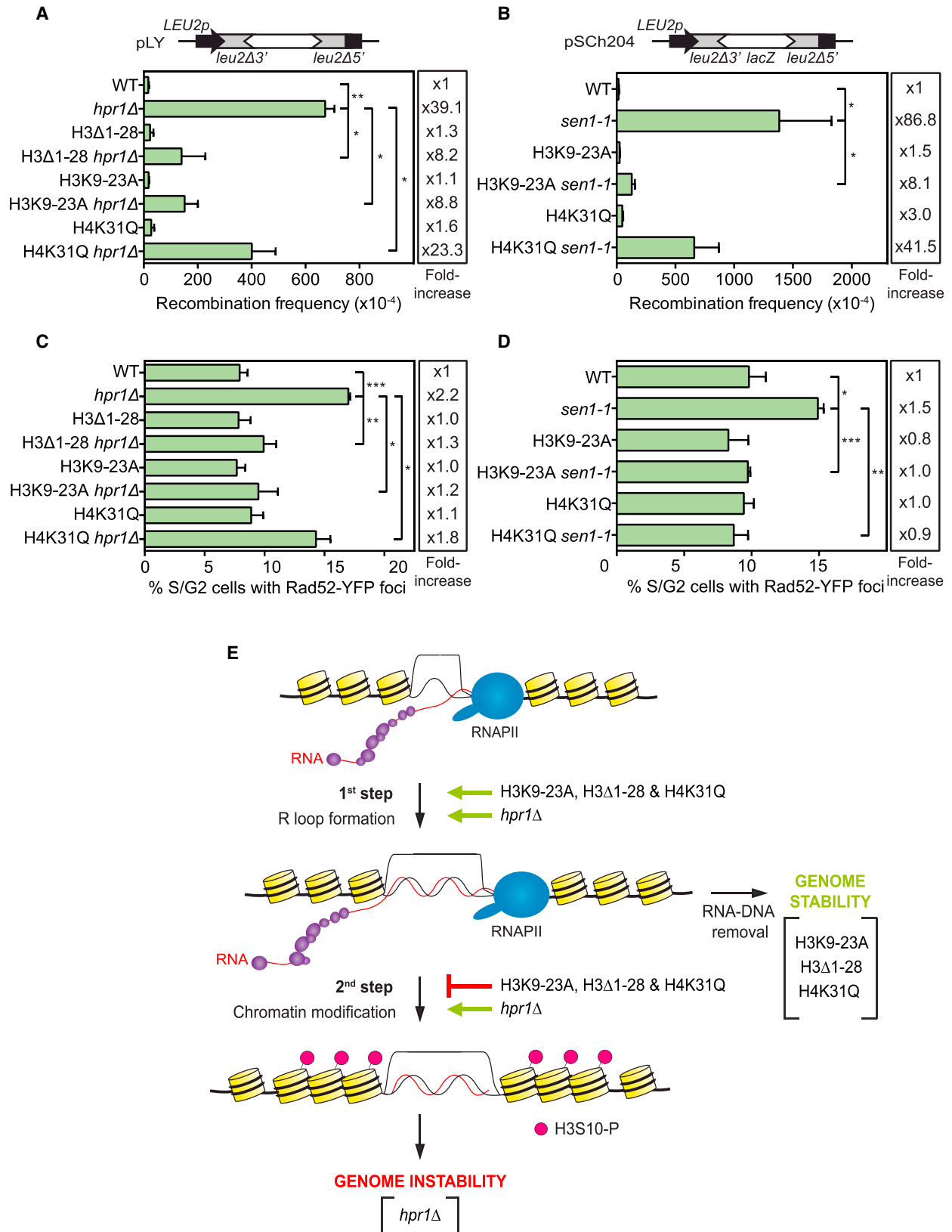
the co-transcriptional dynamics of chromatin in these mutants. Further analysis would be needed to identify the common features that make them R loop prone.

The new types of R loop-accumulating histone mutants identified here uncouple RNA-DNA hybrid formation from genome instability. This chromatin structure, however, facilitates formation of R loops that do not compromise genome integrity. Importantly, the incapacity of the R loops formed in the selected histone mutants to trigger genome instability is not determined by the size of the RNA-DNA hybrids, since they are similar in wild-type cells and in R loop-accumulating mutants (on average 150 bp long with some being larger than 500 bp) regardless of whether they lead to genome instability or not (Figure 4).

(Ferreira et al., 2007; Iwasaki et al., 2011). The slightly lower histone occupancy observed in these mutants, together with the changes in supercoiling of DNA (Figures 5, S5, and S6), suggests a reduction in nucleosome stability and chromatin structure, as previously reported for H3Δ1-28 mutants (Ferreira et al., 2007; Sperling and Grunstein, 2009). The altered chromatin formed in these mutants would facilitate co-transcriptional R loop formation. These data are in agreement with genome-wide analyses showing that R loops are observed in wild-type cells in regions with open chromatin marks and increased DNA accessibility (Sanz et al., 2016). However, a slight decrease in nucleosome occupancy is also observed in H3K9-23R and H4K31R mutants, which do not lead to R loops (Figure S5). This implies that a simple reduction in histone occupancy may not be sufficient to explain the formation of R loops, which may be related with

Therefore, a key question in R loop biology is what differentiates R loops that compromise genome integrity ("bad" R loops) from those that do not ("good" R loops).

Recent reports have shown that R loops that cause genome instability are associated with histone H3S10-P marks and that the chromatin reorganizing complex FACT is required to prevent R loop-dependent transcription-replication conflicts (Castellano-Pozo et al., 2013; Herrera-Moyano et al., 2014). The lack or low level of histone H3S10-P of the H3Δ1-28, H3K9-23A, H3Δ28-31, H3E105Q, H4K5R, H4A15S, H4T82A, H4R95A, and H4K31Q mutants, in contrast to the R loop-dependent hyper-recombinant *hpr1* and *sen1* mutants (Castellano-Pozo et al., 2013), shows, indeed, that H3S10 phosphorylation correlates with harmful R loops. Importantly, H3Δ1-28, H3K9-23A, and H4K31Q mutations suppress the H3S10-P and R loop-mediated instability of *hpr1* and *sen1* mutants, a key result supporting the

A

pLY

LEU2p

leu2Δ3'   *leu2Δ5'*

	Fold-increase
WT	x1
hpr1Δ	x39.1
H3Δ1-28	x1.3
H3Δ1-28 *hpr1Δ*	x8.2
H3K9-23A	x1.1
H3K9-23A *hpr1Δ*	x8.8
H4K31Q	x1.6
H4K31Q *hpr1Δ*	x23.3

Recombination frequency ($\times 10^{-4}$)

B

pSCh204

LEU2p

leu2Δ3' lacZ leu2Δ5'

	Fold-increase
WT	x1
sen1-1	x86.8
H3K9-23A	x1.5
H3K9-23A *sen1-1*	x8.1
H4K31Q	x3.0
H4K31Q *sen1-1*	x41.5

Recombination frequency ($\times 10^{-4}$)

C

	Fold-increase
WT	x1
hpr1Δ	x2.2
H3Δ1-28	x1.0
H3Δ1-28 *hpr1Δ*	x1.3
H3K9-23A	x1.0
H3K9-23A *hpr1Δ*	x1.2
H4K31Q	x1.1
H4K31Q *hpr1Δ*	x1.8

% S/G2 cells with Rad52-YFP foci

D

	Fold-increase
WT	x1
sen1-1	x1.5
H3K9-23A	x0.8
H3K9-23A *sen1-1*	x1.0
H4K31Q	x1.0
H4K31Q *sen1-1*	x0.9

% S/G2 cells with Rad52-YFP foci

E

RNA — RNAPII

1st step — H3K9-23A, H3Δ1-28 & H4K31Q

R loop formation — *hpr1Δ*

RNA — RNAPII

RNA-DNA removal → **GENOME STABILITY**

2nd step — H3K9-23A, H3Δ1-28 & H4K31Q

Chromatin modification — *hpr1Δ*

[H3K9-23A
H3Δ1-28
H4K31Q]

● H3S10-P

GENOME INSTABILITY

[*hpr1Δ*]

(legend on next page)

idea that H3S10-P is necessary for R loop-mediated genome instability. It is worth noting that the non-phosphorylatable H3S10A and phosphomimic H3S10D mutations, previously shown to induce genetic instability (Rad52 foci and plasmid loss) (Castellano-Pozo et al., 2013), were not selected from our AID-induced hyper-recombination screening (Figure 1), implying that they do not form R loops and that the reported genetic instability phenotypes are R loop independent. Consistently, both histone mutations were shown to partially suppress the hyper-recombinant phenotype of *hpr1* (Castellano-Pozo et al., 2013). Therefore, our results demonstrate that H3S10 phosphorylation is a required step for R loops to induce genome instability, even though this does not necessarily mean that H3S10-P by itself is sufficient to cause instability.

It is possible that the ability of an R loop to trigger instability is linked to its ability to promote, once formed, a subsequent chromatin-remodeling step apart from and linked to histone H3 phosphorylation. This modification does not occur in wild-type cells where R loops localize to active chromatin marks (Sanz et al., 2016) and do not induce genome instability. The reason why H3S10 phosphorylation does not occur in the H3 and H4 mutants analyzed (H3K9-23A, H3Δ28-31, H3E105Q, H4K5R, H4A15S, H4T82A, H4R95A, and H4K31Q) is out of the scope of this study, but it is worth noting that a crosstalk between H3S10-P and post-translational modification of K9 or K14 has been previously reported (Rea et al., 2000) and that post-translational modification of histone H4 residues influences H3 modification and vice versa. H4K31 is thus associated with H3 N-terminal tail methylation and H3K4 methylation with H4 acetylation (Kim et al., 2013; Zhang et al., 2015).

In conclusion, this study uncovers a two-step mechanism to explain R loop-mediated genome instability (Figure 7E). In the first step, co-transcriptional R loops are facilitated by a suboptimal chromatin, as suggested by this study, or a defective mRNP biogenesis, as previously reported (Huertas and Aguilera, 2003). In the second step, R loops would elicit modifications in the chromatin by a process that includes H3 serine-10 phosphorylation, to cause genome instability; otherwise, the R loops by themselves would not present a relevant threat to genome integrity. We need to decipher what is different in chromatin dynamics in the selected mutants to become R loop prone and facilitate the first step of our model. However, once formed, R loops may trigger a local chromatin condensation or compaction that would likely constitute a barrier to DNA replication. This is consistent with previous suggestions that chromatin condensation is a cause of chromosome fragility (El Achkar et al., 2005), and with our previous observations that hyper-recombinogenic R loops are linked to H3S10-P in yeast, *C. elegans*, and human cells (Castellano-Pozo et al., 2013), even though this does not exclude that alternative or additional modifications, such H3K9me2 or others, could also contribute to R loop-mediated instability (Castellano-Pozo et al., 2013; Groh et al., 2014; Skourti-Stathaki et al., 2014). Our study, therefore, could give us clues about the difference between "good" (possibly abundant in normal cells) and "bad" R loops (enhanced under pathological conditions), so that only "bad" R loops would be associated with the chromatin modifications responsible for genome instability. Our study thus opens new perspectives to understand the role of RNA-DNA hybrids and epigenetic modifications in the origin of genome instability and cancer.

STAR★METHODS

Detailed methods are provided in the online version of this paper and include the following:

- KEY RESOURCES TABLE
- CONTACT FOR REAGENT AND RESOURCE SHARING
- EXPERIMENTAL MODEL AND SUBJECT DETAILS
  - Yeast strains and media
- METHOD DETAILS
  - Yeast strains
  - Plasmid
  - Large scale yeast transformation
  - Recombination
  - Analyses of Rad52 foci
  - Loss of heterozygosity at the MAT locus
  - Plasmid loss
  - Mutation assays
  - Genotoxic damage sensitivity assay
  - Transcription induction and cell cycle synchronization
  - FACS
  - DRIP assays
  - Bisulfite modification assay
  - Chromatin immunoprecipitation (ChIP)
  - Electrophoresis of DNA topoisomers
- QUANTIFICATION AND STATISTICAL ANALYSIS
- DATA AND SOFTWARE AVAILABILITY

Figure 7. Suppression of *hpr1Δ* and *sen1-1* Genomic Instability by the H3 N-Terminal Tail and H4K31 Mutants

(A) Schematic representation of the direct-repeat recombination system in the pLY plasmid. Recombination frequencies in simple and double *hpr1* and histone mutant strains carrying the pLY plasmid (n = 3).

(B) Schematic representation of the direct-repeat *L-lacZ* recombination system of the pSCh204 plasmid. Recombination frequencies in simple and double *sen1* and histone mutant strains carrying the L-*lacZ* system (n = 4).

(C) Percentage of Rad52-YFP foci formation in simple and double *hpr1* and histone mutants (n ≥ 3).

(D) As in (C) in the simple and double *sen1* and histone mutant strains (n = 4). Means and SEM are plotted in all panels. *p ≤ 0.05; **p ≤ 0.01; ***p ≤ 0.001 (two-tailed Student's t test).

(E) A two-step mechanism model of R loop-mediated genome instability. In the first step, a suboptimal mRNP generation or an altered chromatin favors R loop formation. If they persist, R loops would induce a change in chromatin linked to H3 serine-10 phosphorylation that leads to genome instability. This second step is impeded in H3Δ1-28, H3K9-23A, and H4K31Q mutants.

REFERENCES

Aguilera, A. (2005). Cotranscriptional mRNP assembly: from the DNA to the nuclear pore. Curr. Opin. Cell Biol. *17*, 242–250.

Aguilera, A., and García-Muse, T. (2013). Causes of genome instability. Annu. Rev. Genet. *47*, 1–32.

Aguilera, A., and Klein, H.L. (1988). Genetic control of intrachromosomal recombination in Saccharomyces cerevisiae. I. Isolation and genetic characterization of hyper-recombination mutations. Genetics *119*, 779–790.

Alvaro, D., Lisby, M., and Rothstein, R. (2007). Genome-wide analysis of Rad52 foci reveals diverse mechanisms impacting recombination. PLoS Genet. *3*, e228.

Bhatia, V., Barroso, S.I., García-Rubio, M.L., Tumini, E., Herrera-Moyano, E., and Aguilera, A. (2014). BRCA2 prevents R-loop accumulation and associates with TREX-2 mRNA export factor PCID2. Nature *511*, 362–365.

Castellano-Pozo, M., Santos-Pereira, J.M., Rondón, A.G., Barroso, S., Andújar, E., Pérez-Alegre, M., García-Muse, T., and Aguilera, A. (2013). R loops are linked to histone H3 S10 phosphorylation and chromatin condensation. Mol. Cell *52*, 583–590.

Chan, Y.A., Aristizabal, M.J., Lu, P.Y., Luo, Z., Hamza, A., Kobor, M.S., Stirling, P.C., and Hieter, P. (2014). Genome-wide profiling of yeast DNA:RNA hybrid prone sites with DRIP-chip. PLoS Genet. *10*, e1004288.

Chaudhuri, J., Tian, M., Khuong, C., Chua, K., Pinaud, E., and Alt, F.W. (2003). Transcription-targeted DNA deamination by the AID antibody diversification enzyme. Nature *422*, 726–730.

Chávez, S., and Aguilera, A. (1997). The yeast HPR1 gene has a functional role in transcriptional elongation that uncovers a novel source of genome instability. Genes Dev. *11*, 3459–3470.

Crouch, R.J., Arudchandran, A., and Cerritelli, S.M. (2001). RNase H1 of Saccharomyces cerevisiae: methods and nomenclature. Methods Enzymol. *341*, 395–413.

Dai, J., Hyland, E.M., Yuan, D.S., Huang, H., Bader, J.S., and Boeke, J.D. (2008). Probing nucleosome function: a highly versatile library of synthetic histone H3 and H4 mutants. Cell *134*, 1066–1078.

De Antoni, A., and Gallwitz, D. (2000). A novel multi-purpose cassette for repeated integrative epitope tagging of genes in Saccharomyces cerevisiae. Gene *246*, 179–185.

Domínguez-Sánchez, M.S., Barroso, S., Gómez-González, B., Luna, R., and Aguilera, A. (2011). Genome instability and transcription elongation impairment in human cells depleted of THO/TREX. PLoS Genet. *7*, e1002386.

El Achkar, E., Gerbault-Seureau, M., Muleris, M., Dutrillaux, B., and Debatisse, M. (2005). Premature condensation induces breaks at the interface of early and late replicating chromosome bands bearing common fragile sites. Proc. Natl. Acad. Sci. USA *102*, 18069–18074.

El Hage, A., French, S.L., Beyer, A.L., and Tollervey, D. (2010). Loss of topoisomerase I leads to R-loop-mediated transcriptional blocks during ribosomal RNA synthesis. Genes Dev. *24*, 1546–1558.

Ferreira, H., Somers, J., Webster, R., Flaus, A., and Owen-Hughes, T. (2007). Histone tails and the H3 alphaN helix regulate nucleosome mobility and stability. Mol. Cell. Biol. *27*, 4037–4048.

Gan, W., Guan, Z., Liu, J., Gui, T., Shen, K., Manley, J.L., and Li, X. (2011). R-loop-mediated genomic instability is caused by impairment of replication fork progression. Genes Dev. *25*, 2041–2056.

Garcia, B.A., Hake, S.B., Diaz, R.L., Kauer, M., Morris, S.A., Recht, J., Shabanowitz, J., Mishra, N., Strahl, B.D., Allis, C.D., and Hunt, D.F. (2007). Organismal differences in post-translational modifications in histones H3 and H4. J. Biol. Chem. *282*, 7641–7655.

García-Rubio, M.L., Pérez-Calero, C., Barroso, S.I., Tumini, E., Herrera-Moyano, E., Rosado, I.V., and Aguilera, A. (2015). The Fanconi anemia pathway protects genome integrity from R-loops. PLoS Genet. *11*, e1005674.

Gietz, R.D., Schiestl, R.H., Willems, A.R., and Woods, R.A. (1995). Studies on the transformation of intact yeast cells by the LiAc/SS-DNA/PEG procedure. Yeast *11*, 355–360.

Ginno, P.A., Lott, P.L., Christensen, H.C., Korf, I., and Chédin, F. (2012). R-loop formation is a distinctive characteristic of unmethylated human CpG island promoters. Mol. Cell *45*, 814–825.

Gómez-González, B., and Aguilera, A. (2007). Activation-induced cytidine deaminase action is strongly stimulated by mutations of the THO complex. Proc. Natl. Acad. Sci. USA *104*, 8409–8414.

González-Barrera, S., Prado, F., Verhage, R., Brouwer, J., and Aguilera, A. (2002). Defective nucleotide excision repair in yeast hpr1 and tho2 mutants. Nucleic Acids Res. *30*, 2193–2201.

Groh, M., Lufino, M.M., Wade-Martins, R., and Gromak, N. (2014). R-loops associated with triplet repeat expansions promote gene silencing in Friedreich ataxia and fragile X syndrome. PLoS Genet. *10*, e1004318.

Hatchi, E., Skourti-Stathaki, K., Ventz, S., Pinello, L., Yen, A., Kamieniarz-Gdula, K., Dimitrov, S., Pathania, S., McKinney, K.M., Eaton, M.L., et al. (2015). BRCA1 recruitment to transcriptional pause sites is required for R-loop-driven DNA damage repair. Mol. Cell *57*, 636–647.

Hecht, A., Strahl-Bolsinger, S., and Grunstein, M. (1999). Mapping DNA interaction sites of chromosomal proteins. Crosslinking studies in yeast. Methods Mol. Biol. *119*, 469–479.

Herrera-Moyano, E., Mergui, X., García-Rubio, M.L., Barroso, S., and Aguilera, A. (2014). The yeast and human FACT chromatin-reorganizing complexes solve R-loop-mediated transcription-replication conflicts. Genes Dev. *28*, 735–748.

Hodroj, D., Recolin, B., Serhal, K., Martinez, S., Tsanov, N., Abou Merhi, R., and Maiorano, D. (2017). An ATR-dependent function for the Ddx19 RNA helicase in nuclear R-loop metabolism. EMBO J. *36*, 1182–1198.

Huertas, P., and Aguilera, A. (2003). Cotranscriptionally formed DNA:RNA hybrids mediate transcription elongation impairment and transcription-associated recombination. Mol. Cell *12*, 711–721.

Iwasaki, W., Tachiwana, H., Kawaguchi, K., Shibata, T., Kagawa, W., and Kurumizaka, H. (2011). Comprehensive structural analysis of mutant nucleosomes containing lysine to glutamine (KQ) substitutions in the H3 and H4 histone-fold domains. Biochemistry *50*, 7822–7832.

Kim, K., Lee, B., Kim, J., Choi, J., Kim, J.M., Xiong, Y., Roeder, R.G., and An, W. (2013). Linker histone H1.2 cooperates with Cul4A and PAF1 to drive H4K31 ubiquitylation-mediated transactivation. Cell Rep. *5*, 1690–1703.

Li, X., and Manley, J.L. (2005). Inactivation of the SR protein splicing factor ASF/SF2 results in genomic instability. Cell *122*, 365–378.

Lisby, M., Rothstein, R., and Mortensen, U.H. (2001). Rad52 forms DNA repair and recombination centers during S phase. Proc. Natl. Acad. Sci. USA 98, 8276–8282.

Mason, P.B., and Struhl, K. (2005). Distinction and relationship between elongation rate and processivity of RNA polymerase II in vivo. Mol. Cell 17, 831–840.

Mischo, H.E., Gómez-González, B., Grzechnik, P., Rondón, A.G., Wei, W., Steinmetz, L., Aguilera, A., and Proudfoot, N.J. (2011). Yeast Sen1 helicase protects the genome from transcription-associated instability. Mol. Cell 41, 21–32.

Moriel-Carretero, M., and Aguilera, A. (2010). A postincision-deficient TFIIH causes replication fork breakage and uncovers alternative Rad51- or Pol32-mediated restart mechanisms. Mol. Cell 37, 690–701.

Mumberg, D., Müller, R., and Funk, M. (1994). Regulatable promoters of Saccharomyces cerevisiae: comparison of transcriptional activity and their use for heterologous expression. Nucleic Acids Res. 22, 5767–5768.

Prado, F., and Aguilera, A. (1995). Role of reciprocal exchange, one-ended invasion crossover and single-strand annealing on inverted and direct repeat recombination in yeast: different requirements for the RAD1, RAD10, and RAD52 genes. Genetics 139, 109–123.

Rea, S., Eisenhaber, F., O'Carroll, D., Strahl, B.D., Sun, Z.W., Schmid, M., Opravil, S., Mechtler, K., Ponting, C.P., Allis, C.D., and Jenuwein, T. (2000). Regulation of chromatin structure by site-specific histone H3 methyltransferases. Nature 406, 593–599.

Roca, J. (2009). Two-dimensional agarose gel electrophoresis of DNA topoisomers. Methods Mol. Biol. 582, 27–37.

Santos-Pereira, J.M., and Aguilera, A. (2015). R loops: new modulators of genome dynamics and function. Nat. Rev. Genet. 16, 583–597.

Santos-Pereira, J.M., Herrero, A.B., García-Rubio, M.L., Marín, A., Moreno, S., and Aguilera, A. (2013). The Npl3 hnRNP prevents R-loop-mediated transcription-replication conflicts and genome instability. Genes Dev. 27, 2445–2458.

Sanz, L.A., Hartono, S.R., Lim, Y.W., Steyaert, S., Rajpurkar, A., Ginno, P.A., Xu, X., and Chédin, F. (2016). Prevalent, dynamic, and conserved R-loop structures associate with specific epigenomic signatures in mammals. Mol. Cell 63, 167–178.

Schmittgen, T.D., and Livak, K.J. (2008). Analyzing real-time PCR data by the comparative C(T) method. Nat. Protoc. 3, 1101–1108.

Schwab, R.A., Nieminuszczy, J., Shah, F., Langton, J., Lopez Martinez, D., Liang, C.C., Cohn, M.A., Gibbons, R.J., Deans, A.J., and Niedzwiedz, W. (2015). The Fanconi anemia pathway maintains genome stability by coordinating replication and transcription. Mol. Cell 60, 351–361.

Sikorski, R.S., and Hieter, P. (1989). A system of shuttle vectors and yeast host strains designed for efficient manipulation of DNA in Saccharomyces cerevisiae. Genetics 122, 19–27.

Skourti-Stathaki, K., Kamieniarz-Gdula, K., and Proudfoot, N.J. (2014). R-loops induce repressive chromatin marks over mammalian gene terminators. Nature 516, 436–439.

Smolle, M., and Workman, J.L. (2013). Transcription-associated histone modifications and cryptic transcription. Biochim. Biophys. Acta 1829, 84–97.

Sohail, A., Klapacz, J., Samaranayake, M., Ullah, A., and Bhagwat, A.S. (2003). Human activation-induced cytidine deaminase causes transcription-dependent, strand-biased C to U deaminations. Nucleic Acids Res. 31, 2990–2994.

Sollier, J., Stork, C.T., García-Rubio, M.L., Paulsen, R.D., Aguilera, A., and Cimprich, K.A. (2014). Transcription-coupled nucleotide excision repair factors promote R-loop-induced genome instability. Mol. Cell 56, 777–785.

Sperling, A.S., and Grunstein, M. (2009). Histone H3 N-terminus regulates higher order structure of yeast heterochromatin. Proc. Natl. Acad. Sci. USA 106, 13153–13159.

Sridhara, S.C., Carvalho, S., Grosso, A.R., Gallego-Paez, L.M., Carmo-Fonseca, M., and de Almeida, S.F. (2017). Transcription dynamics prevent RNA-mediated genomic instability through SRPK2-dependent DDX23 phosphorylation. Cell Rep. 18, 334–343.

Stirling, P.C., Chan, Y.A., Minaker, S.W., Aristizabal, M.J., Barrett, I., Sipahimalani, P., Kobor, M.S., and Hieter, P. (2012). R-loop-mediated genome instability in mRNA cleavage and polyadenylation mutants. Genes Dev. 26, 163–175.

Tessarz, P., and Kouzarides, T. (2014). Histone core modifications regulating nucleosome structure and dynamics. Nat. Rev. Mol. Cell Biol. 15, 703–708.

Wahba, L., Amon, J.D., Koshland, D., and Vuica-Ross, M. (2011). RNase H and multiple RNA biogenesis factors cooperate to prevent RNA:DNA hybrids from generating genome instability. Mol. Cell 44, 978–988.

Wahba, L., Costantino, L., Tan, F.J., Zimmer, A., and Koshland, D. (2016). S1-DRIP-seq identifies high expression and polyA tracts as major contributors to R-loop formation. Genes Dev. 30, 1327–1338.

Wellinger, R.E., Prado, F., and Aguilera, A. (2006). Replication fork progression is impaired by transcription in hyperrecombinant yeast cells lacking a functional THO complex. Mol. Cell. Biol. 26, 3327–3334.

Yang, Y., McBride, K.M., Hensley, S., Lu, Y., Chedin, F., and Bedford, M.T. (2014). Arginine methylation facilitates the recruitment of TOP3B to chromatin to prevent R loop accumulation. Mol. Cell 53, 484–497.

Yu, K., Chedin, F., Hsieh, C.L., Wilson, T.E., and Lieber, M.R. (2003). R-loops at immunoglobulin class switch regions in the chromosomes of stimulated B cells. Nat. Immunol. 4, 442–451.

Zhang, T., Cooper, S., and Brockdorff, N. (2015). The interplay of histone modifications—writers that read. EMBO Rep. 16, 1467–1481.

STAR★METHODS

KEY RESOURCES TABLE

REAGENT or RESOURCE	SOURCE	IDENTIFIER
Antibodies		
Rabbit polyclonal anti-H3SS10-P	Millipore	Cat# 06-570; RRID: AB_310177
Rabbit polyclonal anti-Histone H3	Abcam	Cat# ab1791; RRID: AB_302613
Mouse anti-Flag M2	Sigma-Aldrich	Cat# F3165; RRID: AB_259529
Goat anti-Rad53 (yC-19)	Santa Cruz Biotechnology	Cat# sc-6749; RRID: AB_668092
Mouse monoclonal anti-Actin	Abcam	Cat# ab8224; RRID: AB_449644
Mouse monoclonal anti-RNA Pol II (8WG16)	Covance	Cat# MMS-126R; RRID: AB_10013665
S9.6	Hybridoma cell line HB-8730	N/A
Chemicals, Peptides, and Recombinant Proteins		
RNase H	NEB	M0297L
Cycloheximide	Sigma	C7698
Proteinase K	Roche	3115852001
Odyssey blocking buffer	LI-COR	927-40003
Amersham Hybond-XL	GE HEALTHCARE	RPN2020S
iTAq Universal SYBR-green supermix	Biorad	1725125
4–20% CriterioN TGX Precast Midi Protein Gel	Biorad	5671095
Dynabeads Protein A	Thermo Fisher	*10001D*
Alfa-Factor Mating Pheromone	Proteogenix	N/A
Hydroquinone Reagentplus	Sigma	H9003
Toluene	Sigma	244511
N-cetyl-N2-N2-N2-trimethylammonium (CTAB)	Sigma	H6269
PMSF	Sigma	93482
Hydroxyurea	USB Biological	H9120
Zymoliase 20T	USB Biological	Z1000
Chloroquine diphosphate salt	Sigma	C6628
Methyl methanesulfonate	Sigma	129925
Complete Protease Inhibitor Cocktail	Roche	011697498001
Propidium iodide	Sigma	81845
Sodium bisulfite solution	Sigma	13438
Critical Commercial Assays		
QIAquick PCR purification Kit	QIAGEN	28106
Wizard SV Gel and PCR Clean-Up System	Promega	A9282
pGEM-T Easy vector system I	Promega	A1360
NucleoSpin Gel and PCR Clean-up	Macherey-Nagel	740609
Deposited Data		
Raw images	This paper	http://dx.doi.org/10.17632/6pm8g66mdh.1
Experimental Models: Organisms/Strains		
Non Essential Histone H3 and H4 Mutant Collection-Yeast	Dharmacon	YSC5106
A full for a yeast strains is presented in Table S1.	N/A	N/A

(Continued on next page)

Continued

REAGENT or RESOURCE	SOURCE	IDENTIFIER
Oligonucleotides		
A full list of DNA oligos is presented in Table S2.	N/A	N/A
Software and Algorithms		
7500 Software V2.0.6.	Life Technologies	N/A
Multi Gauge V3.0	Fujifilm	N/A
Image Studio V2.1.10	LI-COR	N/A
Prism V6.01	GraphPad	N/A
CellQuest Pro	Becton Dickinson	N/A
ImageJ	NIH Image	N/A

CONTACT FOR REAGENT AND RESOURCE SHARING

Further information and requests for resources and reagents should be directed to and will be fulfilled by the Lead Contact, Andrés Aguilera (aguilo@us.es).

EXPERIMENTAL MODEL AND SUBJECT DETAILS

Yeast strains and media

Yeast strains used in this study are the Non Essential Histone H3 & H4 Mutant Collection from Open Biosystems (Dai et al., 2008) and those listed in the Table S1.

Media used in this study: YPAD (1% yeast extract, 2% peptone, 2% glucose, 20 mg/mL adenine), SD (0.17% yeast nitrogen base without amino acids and ammonium sulfate, 0.5% ammonium sulfate, 2% glucose), SC (SD supplemented with amino acids), SGal (identical to SC but containing 2% galactose instead of glucose), SRaff (identical to SC but containing 2% raffinose instead of glucose), SG/L (identical to SC but containing 3% glycerol and 2% sodium lactate instead of glucose) and SPO (1% potassium acid, 0.1% yeast extract, 0.005% glucose). Solid mediums were prepared adding 2% agar before autoclaving.

Yeast strains were freshly defrosted from stocks and grown at 30°C, except for *sen1-1* strains that was grown at 26°C, using standard practices.

METHOD DETAILS

Yeast strains

The screening and most of experiments were performed with strains form the Non Essential Histone H3 & H4 Mutant Collection from Open Biosystems (Dai et al., 2008). The H3WT and H4WT strains were generated with the collection of H3 and H4 histone mutants by removing one copy of the *HHF-HHT* locus and inserting the reported *URA3* gene near the remaining *HHT* locus in the H3WT and the *HHF* locus in the WTH4. Experiments with synchronized cells and the topoisomer distribution analysis were performed in *bar1*Δ variants (denoted name-B). ChIP and DRIP experiments in the *GAL1::YLR454w* reporter were performed in cells with this construct integrated as previously described (Mason and Struhl, 2005) (denoted name-W). Experiments with the recombination system integrated (Aguilera and Klein, 1988) were performed in cells with this construct (denoted YHT). Experiments with double *hpr1* or *sen1* and histone mutants were performed with strains derived from crossing AWI2C or SEN1-R with the collection strains (denoted YHPK and YSNS respectively). LOH at the MAT locus was performed with the diploid strains denoted YDI.

Plasmid

The pLZGAID plasmid was generated by cloning the *Pvu*II fragment from p414GALAID (Gómez-González and Aguilera, 2007) containing the *GAL1p::AID* fusion into *Nae*I digested pSCh204 plasmid that contains the L-*lacZ* recombination system (Chávez and Aguilera, 1997). This plasmid allows controlled expression of human Activation-Induced Cytidine Deaminase (AID) that deaminates cytidines in the displaced ssDNA strand of R-loops. The *L-lacZ* direct-repeat recombination system is based on two truncated copies of the *LEU2* gene flanking the *lacZ* gene. Recombination reconstitutes the wild-type *LEU2* gene. The pRS317GAL:RNH1 plasmid was generated by cloning the SalI-*Spe*I fragment from pRS315GAL:RNH1 (Huertas and Aguilera, 2003), containing the *GAL1p:RNH1* fusion, into SalI-*Spe*I digested pRS317. The pRS414GALAID-FLAG was generated by in vivo-cloning transforming a wild-type yeast strain with the p414GALAID plasmid (Gómez-González and Aguilera, 2007) and the PCR product obtained with the primers AID-Flag (Table S2) and the pU6H10F plasmid (De Antoni and Gallwitz, 2000). The following plasmids were used: to measure recombination pLY (Prado and Aguilera, 1995) and pSCh204 (Chávez and Aguilera, 1997); plasmid loss pRS414 (Sikorski and Hieter, 1989); Rad52

foci pWJ1344 (Alvaro et al., 2007). To overexpress AID we used p414GALAID and pRS413GALAID (Gómez-González and Aguilera, 2007) and pRS414GAL and pRS413GAL (Mumberg et al., 1994) as no-expression controls. For DNA topoisomer distribution analysis we used pGAL::lacZ (Mumberg et al., 1994).

Large scale yeast transformation
The Non Essential Histone H3 & H4 Mutant Collection was transformed using the lithium acetate method (Gietz et al., 1995), but adapted to 96-well plates. Cells were inoculated in 200 μl 2x YPAD in a flat-bottom 96-well plate using a 96-pin replicator and grown for 2 days at 30°C shaking. Cells were diluted into fresh 2x YPAD media in a round-bottom 96-well plate and incubated 3-4 hr at 30°C shaking. Plates were centrifuged 5 min at 2000 rpm and washed with 150 μl 0.1 M LiAc/10 mM TE. Cells were resuspended in 100 μl prewarmed transformation mix (500 ng plasmid DNA, 90 μl 50% PEG, 100 mM LiAc, 1x TE, 2 μl salmon sperm DNA 6 mg/ml), incubated 30 min at 30°C and 20 min at 43°C. Cells were washed with sterile water and resuspended in 150 μl SC-trp medium. After 2 days at 30°C, 7 μl culture was transferred from the plate into a solid selective media.

Recombination
For recombination assays, cells were grown in SC or SGAL medium plates for 3 to 4 days. Leu+ recombinants of the L-*lacZ* or LY systems were selected on SC-leu-trp or SC-leu-his plates, respectively. His+ recombinants of the chromosomal system were selected on SC-his-lys-leu plates. Recombination frequencies were calculated as the median value of six independent colonies. The average value of three independent transformants was plotted.

Analyses of Rad52 foci
Mid-log cultures of independent transformants carrying pRS315GAL:AID (Leu), pRS317GAL:RNH1 (Lys) or pRS317 (Lys), and pWJ1344 (Trp) containing the *RAD52-YPF* fusion (Alvaro et al., 2007), were fixed with 2.5% formaldehyde and visualized at the fluorescence microscope (NIKON Eclipse NI-E). Spontaneous Rad52-YFP foci were counted from nuclei of S-G2 cells. The average value of three experiments performed with independent transformants was plotted. More than 200 cells were analyzed in each experiment.

Loss of heterozygosity at the MAT locus
In order to study loss of heterozygosity (LOH) at the endogenous MAT locus on chromosome III, we tested the ability of homozygous diploid wild-type and mutant strains to mate with either a *MATa* or a *MATα* mating tester. Mating products were detected by auxotrophy complementation (growth in SD media). Diploid cells (heterozygous at *MAT*) cannot mate due to codominant suppression of haploid-specific cell differentiation pathways. However loss of either *MATa* or *MATα* allele results in the ability to mate with either *MATα* or *MATa*, respectively. Diploid colonies were mated with either F4 or F15 (*MATa* and *MATα*, respectively) mating testers in YPAD for 5 hr and replica-plated to SD plates. The total mated products (with either F4 or F15) were scored by growth on SD. The LOH frequency values (mated products per total cells) are the median of between 4 to 10 independent colonies per strain.

Loss of heterozygosity in this assay might be due to chromosome loss or gene conversion. Chromosome loss was determined in a total of 59 colonies by calculating the ratio of the DNA at the *PRD1* gene (located at the same chromosome as the MAT locus, chromosome III) versus the DNA at the *GCN4* gene (chromosome V). DNA was quantified by quantitative PCR using the comparative Ct method (Schmittgen and Livak, 2008). A ratio below one indicated that chromosome III was lost. A third PCR reaction at the *TRP1* gene, which is in heterozygosis in these diploids, was used as a reference of a gene with only one copy, since the diploid cells were *TRP1+/trp1Δ63*.

Plasmid loss
Colonies of independent transformants carrying the pRS317GAL:RNH1 (Lys) or pRS317 (Lys), pRS315GAL:AID (Leu) and pRS414 (Trp) plasmids were grown in SC-lys-leu or SGAL-lys-leu medium and after 3.5 hr, several dilutions were plated in SC-lys-leu (to score for total cells) and SC-lys-leu-trp (to score for cells which have lost the pRS414 plasmid). Plasmid loss frequencies were calculated as the median value of six independent colonies. The average of three independent transformants is plotted.

Mutation assays
Cells carrying the p414GALAID plasmid were grown in SC-trp or SGAL-trp medium plates for 3 or 5 days. Colonies of independent transformants were grown overnight in SC-trp or SGAL-trp medium, diluted and plated in SC-trp with or without 3 mg/L cyclohex-imide. The mean value of six independent colonies from three independent transformants was represented.

Genotoxic damage sensitivity assay
Mid-log cultures were grown in SC medium. 10-fold dilutions of the culture prepared in sterile water were plated on solid SC medium containing the drugs at the concentrations indicated. UV irradiation was performed in the dried plates. Plates were incubated during 2-6 days (in the dark for UV-irradiated plates).

Transcription induction and cell cycle synchronization

For *GAL1* promoter induction, cells were grown in SG/L medium. Half of the inocule was transferred to 2% galactose-containing medium and the other half to 2% glucose-containing media and grown for 1 hr (no transcription control).

For cell cycle synchronization, overnight cultures were diluted to an OD_{600nm} 0.2 and grown until mid-log phase at 30°C in rich (YPAD) or synthetic medium. Cells were synchronized in G1 adding 0.125 μg/ml of α-factor for *bar1Δ* mutants and 3 μg/ml for *BAR1* cells. After 2.5 hr, cells were released from G1 in the presence or not of 20 mM HU. Samples were taken at the indicated times.

FACS

For FACS analysis, 1 mL of the culture was centrifuged, washed with 1 mL 1x PBS, resuspended in 1 mL 70% ethanol and stored at 4°C. Before the analysis, cells were washed with 1 mL 1x PBS, resuspended in 100 μl RNase A 1 mg/ml in 1x PBS and incubated overnight at 37°C. Next day they cells were washed again with 1x PBS and resuspended in 1 mL of 5 μg/mL Propidium Iodide in 1x PBS, incubated in the dark for 30 min, sonicated 5 s at 10% amplitude and scored in a FACScalibur (Becton Dickinson, CA).

DRIP assays

Cultures were collected, washed with chilled water, resuspended in 1.4 mL spheroplasting buffer (1 M sorbitol, 10 mM EDTA pH 8, 0.1% β-mercaptoethanol, 2 mg/ml Zymoliase 20T) and incubated at 30°C for 30 min. The spheroplasts were pelleted (5 min at 4000 rpm) rinsed with water and homogeneously resuspended in 1.65 mL of buffer G2 (800 mM Guanidine HCl, 30 mM Tris-Cl pH 8, 30 mM EDTA pH 8, 5% Tween-20, 0.5% Triton X-100). Samples were treated with 10 μl 10 mg/ml RNase A for 30 min at 37°C and 75 μl of 20 mg/ml proteinase K (Roche) for 1 hr at 50°C.

DRIP was performed mainly as described (Ginno et al., 2012) with few differences. DNA was extracted gently with chloroform:isoamyl alcohol 24:1. Precipitated DNA was spooled on a glass rod, washed twice with 70% EtOH, resuspended gently in TE and digested overnight with 50 U of *Hind*III, *EcoR*I, *BsrG*I, *Xba*I and *Ssp*I, 2 mM spermidine and 2.5 μl BSA 10 mg/ml. Half of the DNA was treated with 3 μL RNase H (New England BioLabs) overnight 37°C as RNaseH control. Both samples were incubated with 10 μL of S9.6 antibody (1 mg/ml) in 500 μL binding buffer (10 mM NaPO4 pH 7.0, 140 mM NaCl, 0.05% Triton X-100), overnight at 4°C. Hybrid-antibody complexes were immunoprecipitated with 10 μL S9.6 monoclonal antibody that specifically recognize RNA-DNA hybrids coupled to Dynabeads Protein A (Invitrogen) for 2 hr at 4°C and washed 3 times with 1x binding buffer. DNA was eluted in 100 μL elution buffer (50 mM Tris pH 8.0, 10 mM EDTA, 0.5% SDS) treated 45 min with 7 μL proteinase K 20 mg/ml at 55°C and purified with Quiagen DNA purification kit (QIAGEN).

Bisulfite modification assay

DNA from exponentially growing cultures of the indicated strains in YPAD was extracted by the CTAB protocol as described (Moriel-Carretero and Aguilera, 2010). 50 mL of the cultures were collected, washed with 5 mL of chilled water and carefully resuspended in 1 mL of 1M sorbitol-10 mM EDTA pH 8, 0.1% β-mercaptoethanol, 2 mg/mL Zimoliase 20T, and then incubated at 30°C 1h under soft agitation. The pellet (spheroplasts) was washed with 500 μL of cold water and resuspended in 400 μL of cold water. Spheroplasts were lysed by adding 500 μL of CTAB solution (1.4 M NaCl, 100 mM Tris-Cl pH 7.6, 25 mM EDTA pH 8, 2% CTAB). RNA was removed by incubating them 30 min at 50°C with 400 μg of RNase A. Proteins were removed by incubating them with 800 μg of Proteinase K overnight at 30°C under very soft agitation. After centrifugation, pellet and supernatant were treated separately. The supernatant was extracted with 500 μL (24:1) Cloroform:Isoamyl Alcohol. DNA was precipitated with two volumes of 50 mM Tris-Cl pH 7.6, 10 mM EDTA pH 8, 1% CTAB and resuspended in 250 μL 1.4 M NaCl,1 mM EDTA pH 8, 10 mM Tris-Cl pH 7.6. The original pellet was resuspended in 400 μL 1.4 M NaCl, 1 mM EDTA pH 8, 10 mM Tris-Cl pH 7.6 and incubated 1h at 50°C. DNA was extracted with 200 μL (24:1) Cloroform:Isoamyl Alcohol and combined with the DNA obtained from the supernatant. The whole sample was precipitated then with 1vol isopropanol at room temperature, washed with 70% ethanol and resuspended in 100 μL 10 mM Tris-Cl pH 8. DNA was fragmented by digestion with *Nde*I, *Not*I and *Xho*I. The bisulfite modification assay was performed essentially as described (Yu et al., 2003). Genomic DNA was diluted in 42 μL of distilled water with 17.5 μL of 20 mM hydroquinone and 460.5 μL of 2.5 M sodium bisulfite (pH 5.2). The mixture was sealed with mineral oil in a 500 μL microcentrifuge tube and incubated for 16 hr at 37°C in the dark. Bisulfite-treated DNA was purified with the Wizard SV Gel and PCR Clean-Up System (Promega) according to the manufacturer's instructions. Purified bisulfite-treated DNA was desulfonated with 0.3 M NaOH at 37°C for 15 min. Desulfonated DNA was recovered by ethanol precipitation and resuspended in TE (pH 8.0). Bisulfite-modified DNA was used as a template for PCR with either a pair of native primers, or a native primer paired with a 'converted' primer, the sequence of which matched the conversions anticipated owing to deamination of C to U in either the transcribed (TS) or nontranscribed (NTS) strand. PCR bands were purified from agarose gels with the Wizard SV Gel and PCR Clean-Up System (Promega) and cloned in pGEMT-easy. Independent clones were sequenced. Only molecules with more than four consecutive expected C to T changes were considered to determine the R-loop length.

Chromatin immunoprecipitation (ChIP)

ChIP was performed as described (Hecht et al., 1999) with some modifications. For cell extract preparation, pellets were resuspended in 500 μl of lysis buffer (50 mM HEPES-KOH pH 7.5, 150 mM NaCl, 1 mM EDTA pH 8, 1% Triton X-100, 0.1% sodium deoxycholate, 0.1% SDS) supplemented with protease inhibitors (1x Complete Protease Inhibitor Cocktail (Roche) and 1 mM PMSF).

The chromatin was sonicated alternating 1 min high intensity and 20 s rest pulses for 15 min in Bioruptor sonication equipment. Samples were centrifuged for 15 min at 13000 rpm to eliminate cell debris. 30 μl of supernatant were processed as Input and 300 μl were immunoprecipitated.

The immunoprecipitation was performed overnight at 4°C using Dynabeads Protein A (Invitrogen) previously incubated with the antibody for 4 hr rotating at 4°C. Beads were washed as described in Hecht et al. (1999) and chromatin was eluted in 250 μl elution buffer (50 mM Tris-HCl pH 7.4, 10 mM EDTA, 1% SDS) at 65°C for 10 min., treated with 6 μl of 50 mg/ml pronase for 1 hr at 42°C and decrosslinked for 5 hr at 65°C. Quiagen DNA purification kit was used to clean DNA. Real-time quantitative PCR was performed using iTaq universal SYBR Green (Biorad) with a 7500 Real-Time PCR machine (Applied Biosystems).

Electrophoresis of DNA topoisomers

For one-dimensional electrophoresis, DNA was isolated as described (González-Barrera et al., 2002) with few differences. DNA was extracted gently 3 times with phenol:chloroform:isoamyl alcohol 25:24:1, once with chloroform:isoamyl alcohol 24:1 and it was precipitated with isopropanol. DNA was treated with 0.5 μl 10 mg/ml RNase A and incubated for 30 min at 37°C. Finally, DNA was cleaned with chloroform:isoamyl alcohol 24:1, precipitated with isopropanol, washed with 70% ethanol and resuspended in TE. Electrophoresis was carried out in a 0.7% agarose gel with 4 μg/ml chloroquine at room temperature. 30 μg of DNA was loaded in each lane and run in TPE buffer (50 mM Tris-phosphate pH 7.2, 1 mM EDTA, 25 mM phosphoric acid) with 4 μg/ml chloroquine at 40 V for 48 hr. DNA was blot-transferred to a Hybond–XL nitrocellulose membranes (GE Healthcare), which were hybridized with P^{32}-labeled DNA probes.

For two-dimensional electrophoresis, DNA was isolated as described previously (Roca, 2009). For each sample, 40 μg of DNA was loaded in a 0.6% agarose gel TBE buffer with 1 μg/ml chloroquine. The first dimension was run at 45 V for 22 hr at RT (top to bottom). After the first dimension, the gel was soaked in the second dimension electrophoresis buffer containing 5 μg/ml chloroquine for 1 hr and run at 40 V for 14 hr (left to right). DNA was transferred and hybridized as described for 1D gels.

QUANTIFICATION AND STATISTICAL ANALYSIS

Two-tailed Student's t test was performed in all the experiments, with the exception of Figures 6A and 6B, in which Mann-Whitney test was used. The number of experiments (*n*) and *p* values are indicated in corresponding figure legend.

DATA AND SOFTWARE AVAILABILITY

The raw images have been deposited in Mendeley Data and are available at http://dx.doi.org/10.17632/6pm8g66mdh.1.